Proceedings of 2022 IEEE
International Conference on Mechatronics and Automation
August 7 - 10, Guilin China

A Bilateral Six Degree of Freedom Cable-driven Upper Body Exosuit

Jirui Fu[1], Saba M. Hosseini[2], Rylan Simpson[2], Austin Brooks[2], Ryan Huff[1], Joon-Hyuk Park[1**]
[1]Department of Mechanical and Aerospace Engineering
[2]Department of Electrical and Computer Engineering
College of Engineering and Computer Science
University of Central Florida
Orlando FL, 32816 United States
{jerry2020, saba.mhosseini, rylan.simpson, austinbrooks, rchknight99}@knights.ucf.edu
[**]*IEEE Member*, Corresponding Author, joonpark@ucf.edu

2022 IEEE International Conference on Mechatronics and Automation (ICMA) | 978-1-6654-0853-0/22/$31.00 ©2022 IEEE | DOI: 10.1109/ICMA54519.2022.9856241

***Abstract*—The demand for upper limb wearable robots has grown over the past decades across various fields for rehabilitative and assistive applications. While many of this kind have been developed and used in various applications, very few can achieve bimanual task assistance with multiple controlled degrees of freedom (DOF). A bilateral 6-DOF Cable-driven Upper Body Exosuit (CUBE) is presented in this work, designed to aid bimanual tasks via Bowden cable interface to transmit power from actuators placed on the torso to the cuffs on the upper and lower arms. Inertial measurement units (IMUs) and tension sensors are integrated to track the joint angles and cable tension, respectively, to control the position or force exerted through the suit. A preliminary evaluation was performed to assess how CUBE affects the user's effort and performance during bimanual tasks. The results show a reduction in muscle activation from anterior deltoid, medial deltoid, and biceps femoris on both left and right body sides. The benefits of the current design are limited, and the controllers implemented are very basic and low level only, which must be further improved to promote efficient and robust human-robot interactions. Leveraging the current CUBE architecture, our next step is to realize more adaptive and optimal control schemes such as myoelectric and reinforcement learning controls.**

***Index Terms*—Cable-Driven, Wearable Robot, Upper body Exosuit**

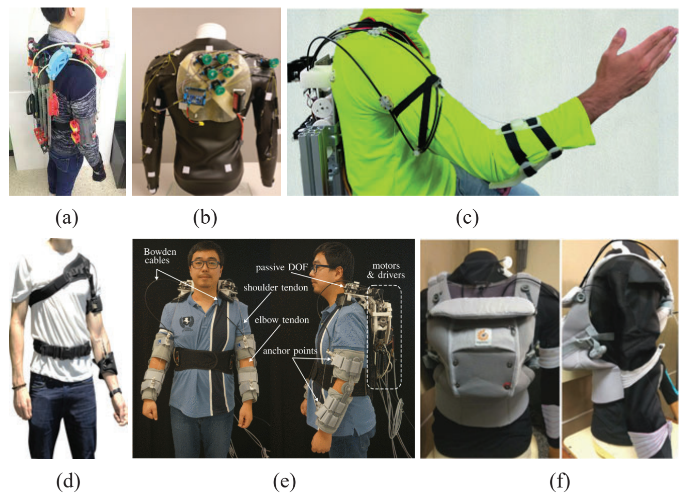

Fig. 1. Various cable-driven upper limb exosuit (a) The Auxilio exosuit for upper limb assistance [5]; (b) The CRUX upper limb exosuit for upper limb rehabilitation [6]; (c) The ExoFlex upper limb exosuit for assistance in elbow and shoulder rehabilitation therapies [7]; (d) The adaptive cable-driven exosuit for elbow rehabilitation [8]; (e) The upper limb exosuit for industrial applications [9]; (f) A cable driven upper limb exosuit for elbow and shoulder assistance [3]

I. Introduction

Upper limb wearable robots are designed to provide assistance to help reduce physical efforts and fatigue, or increase the endurance and performance of the upper limbs [1]. Further, upper limb wearable robots are used in rehabilitation to assist impaired individuals in performing activities of daily living [2]. More recently, most designs have adopted soft materials and flexible interfaces to enhance wearability and ergonomics, and to reduce the body-borne load, commonly referred to as an exosuit [3]. These exosuit designs have significantly advanced user compliance, practicality and usability over recent years [4].

Existing upper limb exosuits commonly employ cable-driven mechanisms due to their advantages of being lightweight, low inertia imposed on the moving limbs, and added versatility in component placement, such as motors and batteries [10]. Many upper limb exosuit designs introduced in recent years take different architectures and control methods.

The exosuit shown in Fig. 1(a) iis a 3-DOF unilateral exosuit for upper body rehabilitation, which is controlled by a low-level PID controller to guide the users arm to follow a predefined motion trajectory [5]. However, it lacks the capability to support the bimanual motion. A 6-DOF unilateral cable-driven exosuit was designed to augment the arms controlled by a PID position controller (Fig. 1(b)) [6]. The exosuit shown in Fig. 1(c) assists shoulder and elbow flexion controlled by a PD controller to assist the user in moving arms to the desired position [7], but its hardware is not integrated within the exosuit. There is an exosuit which implements myoelectric control scheme for power augmentation of elbow (Fig. 1(d)) [8]. Similarly, an exosuit with bimanual function is designed

(Fig. 1(e)) which can assist the elbow and shoulder flexion using the users voice input [9]. An exosuit shown in Fig. 1(f) assists shoulder and elbow flexion but lacking bimanual function [3]. Most of these different designs of upper limb exosuits is not capable of bilateral shoulder and elbow assistance. Hence, a 6DOF Cable-driven Upper Body Exosuit (CUBE) has been developed to reduce the users effort by assisting elbow and shoulder joints bilaterally. Further, we incorporate soft materials with 3D printed parts to achieve a lightweight, ergonomic, and wearable interface. CUBE integrates inertial measurement units (IMUs) to track the user's arm motion and tension sensor for closed-loop control of the assistive force modulated by six motors. The control system can aid in predefined motion tasks or reduce joint load by providing external forces on the elbow and shoulders through cable actuation. The pilot testing was performed to assess the error-tracking performance, wearability, and reduction in human effort.

In the following sections, the overall design of CUBE is explained (section II), the dynamic modeling and control are covered (section III), and the preliminary experiment and results are presented (section IV). Finally, the challenges and future directions are given in the last section.

II. System Design and Modeling

A. System Architecture

CUBE consists of a mechanical and an electrical subsystem (Fig. 2). The mechanical subsystem comprises arm braces, shoulder mounts, and cable transmissions. The electrical subsystem comprises DC motors, tension sensors, IMUs, and a single-board computer.

The primary design consideration was the use of the cable-driven system. Much of the design decisions revolve around routing the cable and directing the force to the user's arm. The cables help transfer force without interfering the motion of the joints. When the exosuit is disabled, the user can achieve unrestricted motion of their arms. The cable-based power transmission offers lightweight and low-profile interface, thereby improve the wearability. A 3D CAD model of the CUBE is shown in Fig. 3, designed to assist 3 DOF in each arm: shoulder flexion and abduction, and elbow flexion

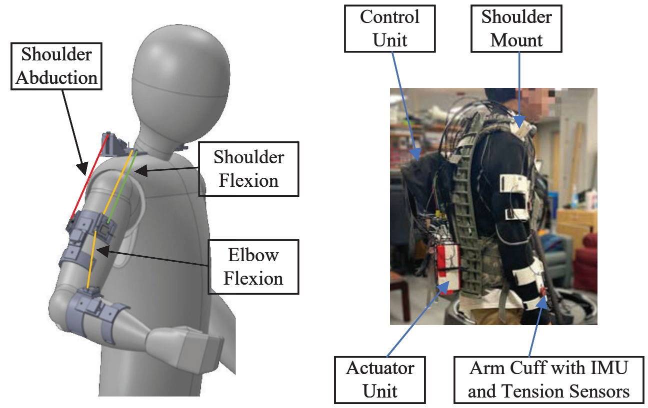

(a) (b)

Fig. 3. (a) The CAD model of the upper limb cable-driven bilateral exosuit; (b) The CUBE exosuit from the side view.

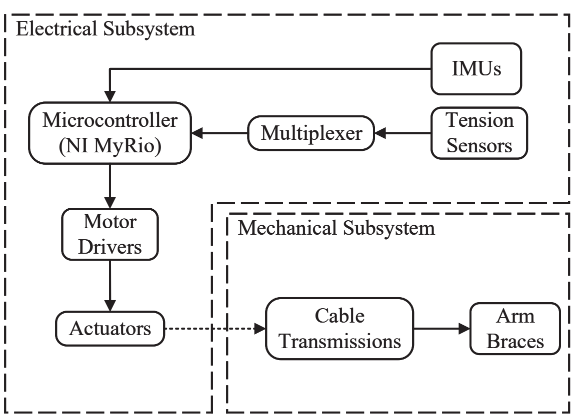

Fig. 2. The System Diagram of the 6-DOF cable driven bilateral upper limb exosuit

The upper limb exosuit comprises four cuffs a forearm cuff and an upper arm cuff on each side. Two shoulder mounts and six cables are routed through these cuffs and actuators. Four cables terminate at two upper arm cuffs, which control the 2-DOF motion on the shoulder joint. The shoulder mount is a crucial part to guide the cables to each degree of freedom, hence optimized for its position and angle (Fig. 4(a)). Remaining two cables terminate at two forearm cuff which control the 1-DOF motion on the elbow joint. The arm cuffs were 3D printed using Polylactic acid (PLA) with mounts for the tension sensors and IMUs, and velcro straps for tightening (Fig. 4(b)).

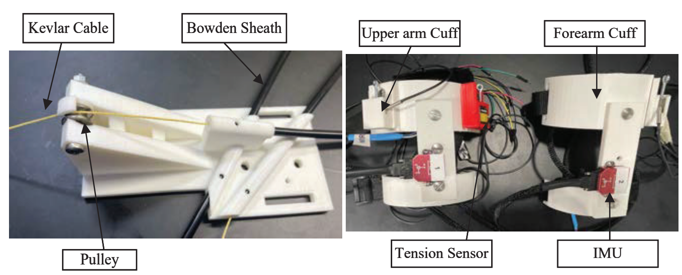

(a) (b)

Fig. 4. (a) The shoulder mount routed with Bowden sheath and Kevlar cable; (b) The left and right arm cuff with IMU and tension sensor installed.

B. Kinematic Model of CUBE

The kinematic model of the arm was developed using Denavit-Hartenberg (DH) parameters described in Table I. The q_1,q_2 and q_3 are the joint angles of each assisted joint. The model is illustrated in Fig. 5 which depicts R-R-R kinematics.

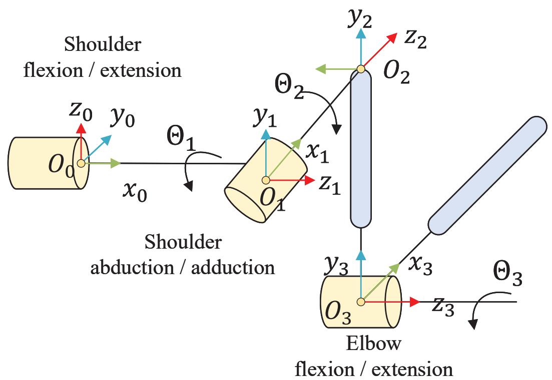

Fig. 5. The Kinematic scheme of the three degree-of-freedom human arm. The angles θ_1, θ_2, and θ_3 are the shoulder flexion, shoulder abduction, and elbow flexion corresponds to the q_1, q_2, and q_3 in Table. I

TABLE I
D-H PARAMETER OF THE EXOSUIT

Link	a_i	α_i	d_e	q_e	Motion
1	0	$\frac{\pi}{2}$	0	q_1	Shoulder Flexion
2	0	$\frac{\pi}{2}$	l_1	q_1	Shoulder Abduction
3	0	0	l_2	q_2	Elbow Flexion

C. Gometric Model of CUBE

The geometric model of CUBE was developed based on the cable attachment points on the human arm in order to relate the cable length to the respective joint kinematics, and cable force to the respective joint torque. As illustrated in Fig. 6 (c), the shoulder abduction-adduction model and shoulder flexion-extension model shares the same geometric characteristics, hence represented as the same. $\left|\overrightarrow{E_iC_i}\right|$ and $\left|\overrightarrow{S_iP_i}\right|$ depicts the offset from the body segment centerline to the cable attachment points. $\left|\overrightarrow{C_iO_i}\right|$ depicts the distance between the cable attachment point projected on the segment centerline and the joint center. $\left|\overrightarrow{P_iO_i}\right|$ depicts the offset from the joint center to the Bowden cable mount projected on the segment centerline. The objective of this geometric model is to define the kinematics relationship between the cable length ($\left|\overrightarrow{E_iS_i}\right|$) and the joint angle ($q_i$), and the angle ϕ_i which is needed to map the cable force to the joint torque. The parameters in the geometric model of each DOF are presented in Table II where all parameters except joint angle q_i are constant.

TABLE II
THE KNOWN GEOMETRIC PARAMETERS OF EACH DOF

Motion	i	$\left\|\overrightarrow{E_iC_i}\right\|$	$\left\|\overrightarrow{C_iO_i}\right\|$	$\left\|\overrightarrow{P_iO_i}\right\|$	$\left\|\overrightarrow{S_iP_i}\right\|$	q_i
Shoulder Flexion	1	h_u	l_1	h_1	d_1	q_1
Shoulder Abduction	2	h_u	l_2	h_2	d_2	q_2
Elbow Flexion	3	h_f	l_3	h_3	h_u	q_3

The angle $\angle S_iE_iO_i$ is the sum of the angle between the cable and arm (ϕ_i) and $\angle G_iE_iO_i$. Consistent with the human arm geometry, $\overrightarrow{E_iG_i}$ is parallel to $\overrightarrow{C_iO_i}$(the axis along the

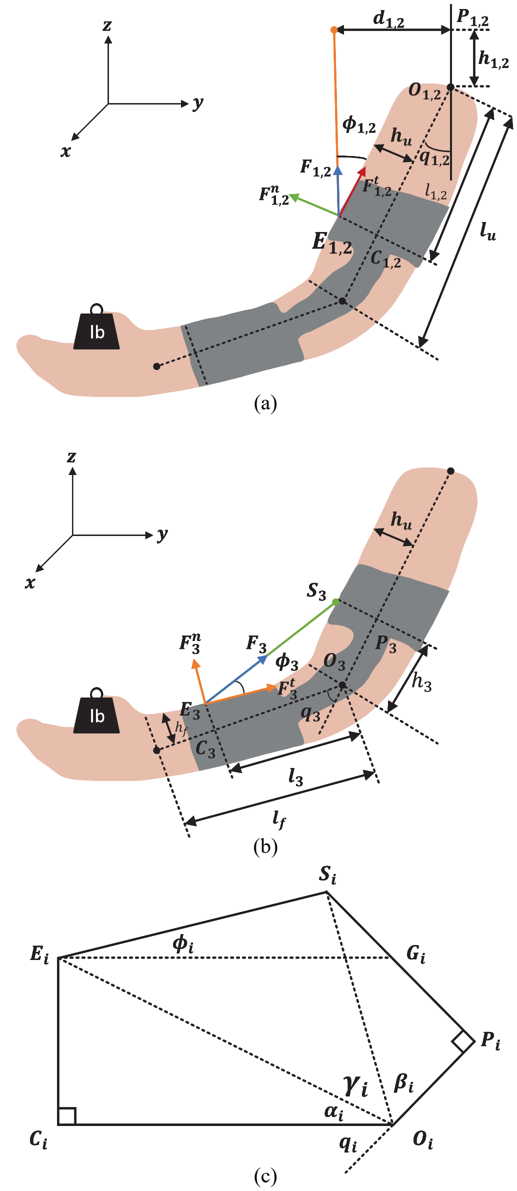

Fig. 6. (a) The free body diagram for the DOF on shoulder joint which includes shoulder flexion and shoulder abduction; (b) The free body diagram for the DOF on the elbow joint which only includes elbow flexion; (c) The geometric model between the cable and human arm which is feasible for all DOFs of the CUBE.

forearm or upperarm). Therefore, $\angle G_iE_iO_i$ equals to α_i defined in (1).

$$\alpha_i = tan^{-1}\frac{\left|\overrightarrow{E_iC_i}\right|}{\left|\overrightarrow{C_iO_i}\right|} \tag{1}$$

According to the Sine Law, $\angle S_iE_iO_i$ can be expressed as (3).

$$\frac{\overrightarrow{|S_iO_i|}}{sin(\angle S_iE_iO_i)} = \frac{\overrightarrow{|E_iS_i|}}{sin(\gamma_i)} \tag{2}$$

$$\angle S_i E_i O_i = sin^{-1} \frac{\left|\overrightarrow{S_i O_i}\right| sin(\gamma_i)}{\left|\overrightarrow{E_i S_i}\right|} \tag{3}$$

$$\phi_i = \angle S_i E_i O_i - \alpha_i \tag{4}$$

Where the γ_i is a function of the joint angle q_i.

$$\gamma_i = \pi - q_i - \alpha_i - \beta_i \tag{5}$$

Where the α_i is derived from the (1), and β_i is calculated as below,

$$\beta_i = tan^{-1} \frac{\left|\overrightarrow{S_i P_i}\right|}{\left|\overrightarrow{P_i O_i}\right|} \tag{6}$$

The $\left|\overrightarrow{E_i O_i}\right|$ and $\left|\overrightarrow{S_i O_i}\right|$ are constant values obtained as below.

$$\left|\overrightarrow{E_i O_i}\right| = \sqrt{(\left|\overrightarrow{E_i C_i}\right|)^2 + (\left|\overrightarrow{O_i C_i}\right|)^2} \tag{7}$$

$$\left|\overrightarrow{S_i O_i}\right| = \sqrt{(\left|\overrightarrow{S_i P_i}\right|)^2 + (\left|\overrightarrow{P_i O_i}\right|)^2} \tag{8}$$

The length of $\overrightarrow{E_i S_i}$ can be obtained using trigonometric identities (9). This completes the kinematics relationship between cable length and joint motions.

$$\left|\overrightarrow{E_i S_i}\right|^2 = \left|\overrightarrow{E_i O_i}\right|^2 + \left|\overrightarrow{S_i O_i}\right|^2 - 2\left|\overrightarrow{E_i O_i}\right|\left|\overrightarrow{S_i O_i}\right| cos(\theta_i) \tag{9}$$

The cable force to joint torque relationship (10) is also easily obtained using the angle ϕ_i which is a function of joint angle q_i.

$$\tau_i = F_i sin(\phi_i)(l_i) \tag{10}$$

D. Dynamic Model of CUBE

The dynamic model of the arm was developed for sagittal and coronal plane, respectively (Fig. 6(a), (b), & (c)). The following assumptions were made to simplify the model, acting in the sagittal and coronal planes.

1) The load on the hand is assumed to be a point mass acting on the endpoint of the hand (the center of the palm).
2) The changes in the inertia of forearm and the load due to different elbow joint angle have negligible effect on shoulder abduction/adduction dynamics.
3) Axial rotation of the upper arm and forearm can be accommodated within the cuff interface and does not significantly alter the geometry of the developed model.

The equation of motion of the exosuit is derived from Euler-Lagrange's Method. The general coordinates are q_i is the joint angle vector $[q_1,\ q_2,\ q_3]^T$, where q_1 represents the shoulder flexion, q_2 represents the shoulder abduction, and q_3 represents the elbow flexion. The dynamic model is expressed as 11, where D(q) is inertia matrix which is a 3×3 symmetric and positive definite matrix for each $q \in R^3$, $C\left(q,\ \dot{q}\right)$ is the vector of Coriolis, $g(q)$ is the gravity term, τ_r: is the torque vector exerted by the robot on elbow flexion, shoulder flexion and shoulder abduction; τ_h: is the torque vector exerted by the user on elbow flexion, shoulder flexion and shoulder abduction which represents the amount of the users effort.

$$\tau + \tau^h = M(q)\ddot{q} + C(q,\dot{q})\dot{q} + g(q) \tag{11}$$

III. Electrical and Control System

A. Electrical System

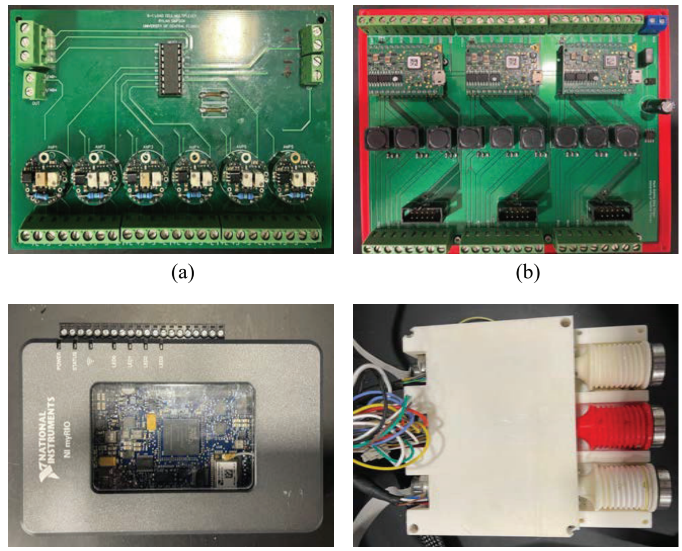

(a) (b) (c) (d)

Fig. 7. (a) The PCB designed for the multiplexer and amplifiers; (b) The PCB designed for the motor driver; (c) The National Instrument MyRio-1900 implemented in the CUBE; (d) The actuator box for one side

The electrical system consists of the sensing, actuation, and control modules. The sensing module includes five IMUs (VectorNav VN-100) to measure the joint angles and six tension sensors (Futek LSB-200) to measure the tension on each Bowden cable. Four IMUs are installed on each cuff, while one is installed at the center of the torso. All the tension sensors are housed and secured within the arm cuffs. The cables are connected to the tension sensor by eye bolts. The signal of tension sensors are amplified by strain gauge amplifiers (Mantracourt ICA1H) then multiplexed (Vishay DG408) into a single analog channel. A custom Printed Circuit Board (PCB) was designed to include all six amplifiers and one multiplexer to reduce the overall size of the electronic hardware (Fig.7 (a)). Six Maxon EC-i 30W motors were used for the actuation module. These motors are driven by 6 separate ESCON Module 24/2 motor drivers placed on two custom-made PCBs (Fig.7 (b)) to reduce the size and weight of the electronics. The motor drivers are configured as a current controller to set the motor's output torque. In addition, each motor has a 512-count quadrature encoder to track the cable displacement and speed. The head of each motor has a winch that winds the cables (Fig.7 (d))

The exosuit is controlled by the National Instruments (NI) myRIO-1900, a microcontroller with a built-in Xilinx FPGA (Fig.7 (c)).The FPGA is responsible for all low-level data acquisition and control of the motors, tension sensors, and IMUs. A graphical user interface (GUI) was developed using LabVIEW to monitor real time sensor data and to control CUBE 8).

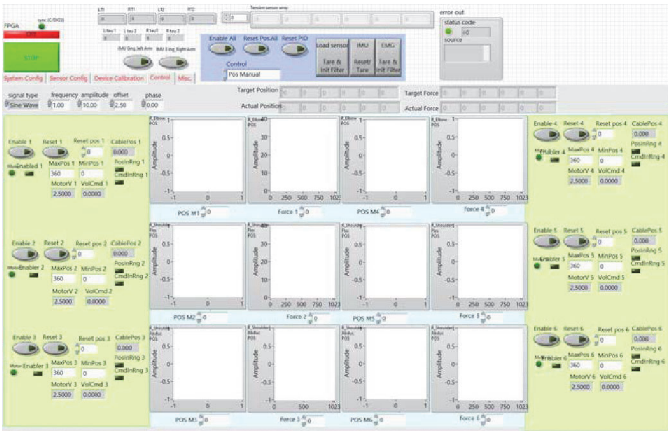

Fig. 8. The screenshot of the user interface of the LabVIEW program designed for the CUBE exosuit. The User can select the control mode from the drop-down list and input the desired position or force in this user interface

B. Control System

1) Position Control Mode: Two control modes were implemented: position control and force control. The position control mode assists the user in keeping the arm at a constant posture while carrying a load or to guide the user's arm on a predefined path. This mode utilizes the IMUs to track the angle of the human arm's joints, and the encoder to track the length of the cable. The calibration posture of position control mode is arm straight down to put palms on thighs during which the initial angle (0^o) is set for elbows and shoulders. The motor shaft position is also zeroed during this process to start tracking cable displacements. To use the position control mode, the user must start from the predefined initial position where the angles of all assisted joints must be zero. When the user starts moving the arm from the initial position, the IMU sensors track the angle of the body joints, then convert the joint angles to the corresponding cable length using the geometric relationship described in II. C. Denoting $L(q)$ as the cable length expressed as a function of joint angle q, the above-mentioned is expressed in (12), where q_0 is the vector of initial joint angles.

$$\Delta L(q) = L(q) - L(q_0) \tag{12}$$

where $L(q)$ is the length of the cable corresponds to the measured joint angle. The difference $\Delta L(q)$ is the input to the actuator controller with the goal of controlling cable length to reach $L(q)$. The controller consists of a, a lower-level actuator current controller, and an encoder. The difference between the targeted and actual length of winded cable is mapped to the

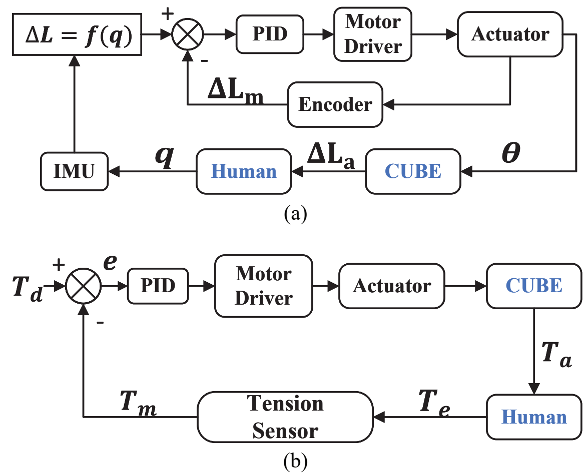

Fig. 9. (a) The block diagram for the position control system of the CUBE; (b) The block diagram for the position control system of the CUBE.

control command of the PID position controller, then fed into the lower-level actuator current controller to wind the cable by rotating a motor shaft and winch. While winding the cable, the encoder at the feedback loop counts the angular displacement of the actuator and maps the measurement to the actual length of the winding cable ($\Delta L_a(t)$). Then, the input to the PID controller is updated based on the result from the feedback loop.

$$e(t) = \Delta L(t) - \Delta L_a(t) \tag{13}$$

$$u(t) = k_p e(t) + k_I \int e(t)dt + k_D \frac{de(t)}{dt} \tag{14}$$

The input of the PID position controller consists of a vector which is $\Delta L\,(q) \in \mathbb{R}^3$. Therefore, the controller is a MIMO (multi-input and multi-output) type controller. The gains of the PID position controller are same among the joints in which k_p, k_i and k_d are set at 0.4, 1, and 0,001, respectively.

2) Force Control Mode: The force control mode can modulate the cable tension and is designed to output a controlled assistive force at the targeted joints to reduce the users work. The force control system implements the tension sensor as feedback and a PID controller to map the input to the control command of lower-level actuator control (Fig. 9 (b)). The desired cable tension T_d is the input to the PID controller which maps the difference between desired cable tension and actual cable tension to control the output tension. The PID gains of the force control, i.e., k_p, k_i, and k_d with values of 0.13, 0.5, and 0.0001, respectively, are the same across the joints.

IV. Results

A pilot study was conducted (1 male, weight 60.8 kg, height 182 cm, age 19) to evaluate the effect of CUBE during a bimanual load-carrying task. The experiment was performed in two conditions, assisted and unassisted modes. The subject wore the exosuit and performed repetitive shoulder flexion, shoulder abduction, and elbow flexion movements within 4 seconds while holding a 5.5 lbs. dumbbell in hand. The ranges of elbow flexion and shoulder flexion were between 0^o to 70^o, and the range of shoulder abduction was controlled to be between 0^o to 45^o. The surface electromyography (sEMG) electrodes (MyoMuscle, Noraxon, USA) were placed on biceps, anterior deltoid, mid deltoid on both arms to measure muscle activation with or without the assistance provided by CUBE. The sEMG signal was measured at a 2 kHz sampling rate. The collected sEMG signal was processed using a band-pass filter with a low cut-off frequency of 20 Hz and a high cut-off frequency of 450 Hz to remove the noise and artifacts in the raw surface EMG signal, full wave rectified, and was then smoothed by a lowpass filter with a cut-off frequency of 6 Hz. [11]. Finally, the filtered sEMG was normalized by the Maximum Voluntary Contraction (MVC) of the subject. Fig. 13 shows the results of EMG data presented as a % of MVC during elbow flexion (data collected from bicep brachii), shoulder flexion (data collected from anterior deltoid) and shoulder abduction (data collected from medial deltoid), with and without the assistance.

The results showed that the exosuit reduced the muscle effort by 17.76% and 16.42% in left and right anterior deltoids, 14.70% and 4.71% in left and right mid deltoids, and 7.18% and 15.43% in left and right bicep brachii, during shoulder flexion, shoulder abduction, and elbow flexion, respectively (Table III). However, the percentage reduction of muscle activation between the left and right arms showed a considerable difference in elbow flexion and shoulder abduction. This might have been due to a difference in muscle mass and strength between left and right arm, and also couldve been caused by a slight change in the position and orientation of the cuffs during testing, impacting the accuracy of the geometric model.

TABLE III
MUSCULAR ERROFT REDUCTION ON THE BICEPS BRACHII AND ANTERIOR DELTOID

ELBOW FLEXION	
Left Biceps Brachii (%)	Right Biceps Brachii (%)
7.18%	15.43%
SHOULDER FLEXION	
Left Anterior Deltoid (%)	Right Anterior Deltoid (%)
17.76%	16.42%
SHOULDER ABDUCTION	
Left Mid Deltoid (%)	Right Mid Deltoid (%)
14.7%	4.71%

V. DISCUSSION

The preliminary results suggest that CUBE does reduce arm muscle work. However, to what extent and how effectively during more complex bimanual tasks should be more thoroughly examined. Moreover, the benefit of using CUBE should outweigh the added weight of carrying the hardware by the user. The control schemes implemented on CUBE are very basic and not suitable to facilitate efficient and robust

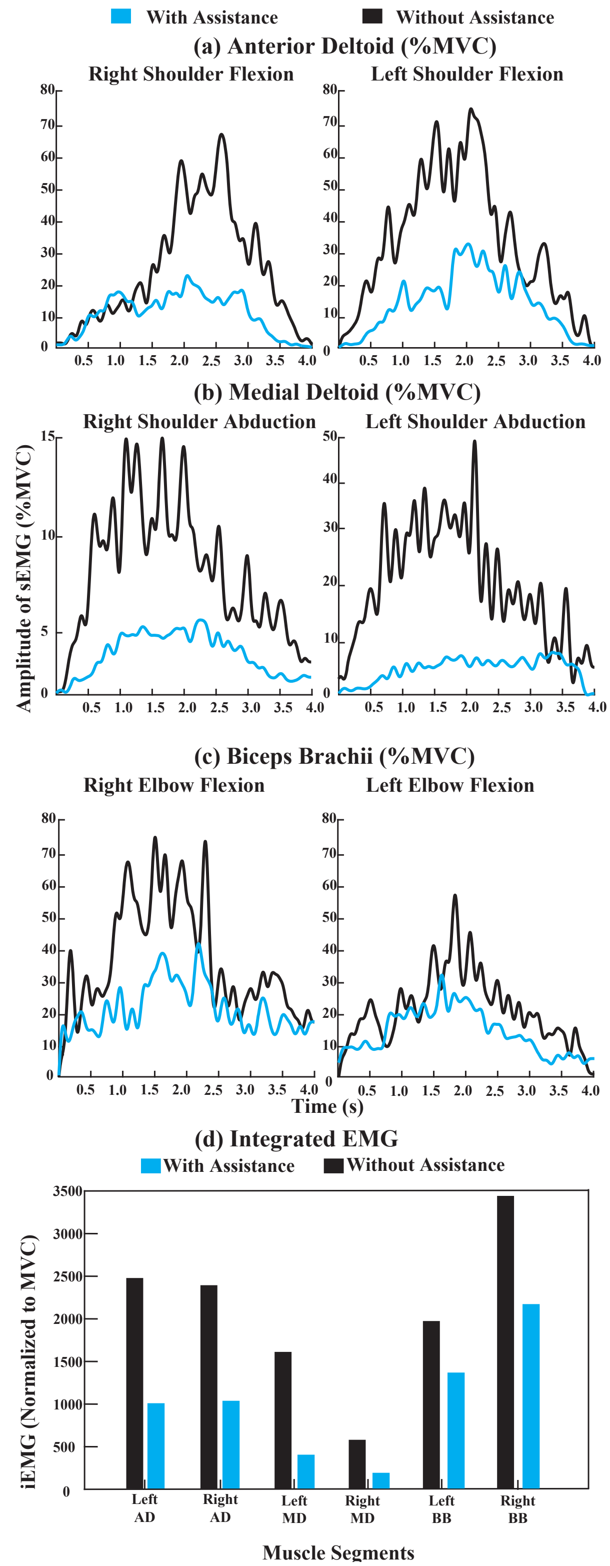

Fig. 10. Experiment results showing sEMG data collected from (a) anterior deltoid, (b) medial deltoid, (c) bicep brachii, and (d) barplots comparing integrated sEMG values under two conditions, with and without CUBE assistance. The x axis displays time in seconds, while the y axis shows the sEMG normalized to % MVC.

assistance and human-robot interaction. Thus, future work will be focused on developing more advanced control schemes to implement on CUBE, such as myoelectric control using surface EMG signals as control inputs for motion intention and load detection. To enhance the actuation and control performance using cable-based power transmission, adding compliance using springs [12] or an adaptive compensator [13] will be sought. Furthermore, the current CUBE design only supports unidirectional motions. Therefore, motions such as shoulder extension, elbow extension, and shoulder adduction are not controlled nor assisted. In the next version of the CUBE design, antagonistic actuation using two cables connected to a single pulley (motor) will be implemented to achieve bi-directional joint assistance. The testing and evaluation of CUBE should be done on a large group of people to demonstrate the efficacy and performance, for which a human subject study protocol is currently underway to be approved by the UCF Institutional Review Board (IRB).

VI. Conclusion

This work presents a 6-DOF bilateral cable-driven upper body exosuit (CUBE) to aid the user in bimanual tasks. This exosuit can be controlled by either the position mode or the force mode. A pilot test was conducted showing reduction in elbow and shoulder flexor muscle, and shoulder abductor muscle activations while using CUBE. Although the current design and control of CUBE present areas that must be further improved and optimized, the presented work is a critical step toward investigating efficient control strategies for bilateral arm exosuit through the implementation of the more adaptive and optimal control schemes, such as myoelectric control and reinforcement learning control.

References

[1] B. Treussart, F. Geffard, N. Vignais, and F. Marin, "Controlling an upper-limb exoskeleton by emg signal while carrying unknown load," in *2020 IEEE International Conference on Robotics and Automation (ICRA)*, B. Treussart, F. Geffard, N. Vignais, and F. Marin, Eds., 2020, Conference Proceedings, p. 7.

[2] G. Riva and E. Riva, "Retrainer: An exoskeleton-based rehabilitation system for stroke patients," *Cyberpsychology, Behavior, and Social Networking*, vol. 23, no. 4, p. 271272, 2020.

[3] J. L. Samper-Escudero, A. Gimenez-Fernandez, M. A. Sanchez-Uran, and M. Ferre, "A cable-driven exosuit for upper limb flexion based on fibres compliance," *IEEE ACCESS*, vol. 8, p. 153297153310, 2020.

[4] J. C. Perry, J. Rosen, and S. Burns, "Upper-limb powered exoskeleton design," *IEEE/ASME Transactions on Mechatronics*, vol. 12, no. 4, pp. 408–417, 2007.

[5] I. Gaponov, D. Popov, S. J. Lee, and J.-H. Ryu, "Auxilio: A portable cable-driven exosuit for upper extremity assistance," *International Journal of Control, Automation and Systems*, vol. 15, no. 1, pp. 73–84, 2017. [Online]. Available: https://doi.org/10.1007/s12555-016-0487-7

[6] S. Lessard, P. Pansodtee, A. Robbins, L. B. Baltaxe-Admony, J. M. Trombadore, M. Teodorescu, A. Agogino, and S. Kurniawan, "Crux: A compliant robotic upper-extremity exosuit for lightweight, portable, multi-joint muscular augmentation," in *2017 International Conference on Rehabilitation Robotics (ICORR)*, 2017, pp. 1633–1638.

[7] D. Pont, A. F. Contreras, J. L. Samper, F. J. Sez, M. Ferre, M. . Snchez, R. Ruiz, and . Garca, "Exoflex: An upper-limb cable-driven exosuit," in *Robot 2019: Fourth Iberian Robotics Conference*. Springer International Publishing, 2019, Conference Proceedings, pp. 417–428.

[8] N. Lotti, M. Xiloyannis, G. Durandau, E. Galofaro, V. Sanguineti, L. Masia, and M. Sartori, "Adaptive model-based myoelectric control for a soft wearable arm exosuit: A new generation of wearable robot control," *IEEE Robotics & Automation Magazine*, vol. 27, no. 1, pp. 43–53, 2020.

[9] Y. G. Kim, M. Xiloyannis, D. Accoto, and L. Masia, "Development of a soft exosuit for industrial applications," in *2018 7th IEEE International Conference on Biomedical Robotics and Biomechatronics (Biorob)*, 2018, Conference Proceedings, pp. 324–329.

[10] J. D. Sanjuan, A. D. Castillo, M. A. Padilla, M. C. Quintero, E. E. Gutierrez, I. P. Sampayo, J. R. Hernandez, and M. H. Rahman, "Cable driven exoskeleton for upper-limb rehabilitation: A design review," *Robotics and Autonomous Systems*, vol. 126, 2020.

[11] W. Rose, "Electromyogram analysis," p. 10, 2011. [Online]. Available: https://www1.udel.edu/biology/rosewc/kaap686/notes/EMG%20analysis.pdf

[12] A. Schiele, P. Letier, R. V. D. Linde, and F. V. D. Helm, "Bowden cable actuator for force-feedback exoskeletons," in *2006 IEEE/RSJ International Conference on Intelligent Robots and Systems*, 2006, Conference Proceedings, pp. 3599–3604.

[13] B. K. Dinh, M. Xiloyannis, C. W. Antuvan, L. Cappello, and L. Masia, "Hierarchical cascade controller for assistance modulation in a soft wearable arm exoskeleton," *IEEE Robotics and Automation Letters*, vol. 2, no. 3, pp. 1786–1793, 2017.